doi: 10.13241/j.cnki.pmb.2022.05.032

胸部 CT 结合 AI 诊断系统对疑似肺结节患者的诊断及对结节类型的评估价值 *

刘亚斌 李 庆 周 围 郑常俊 舒 亚

（成都医学院第一附属医院放射科 四川 成都 610500）

摘要 目的：探讨胸部 CT 结合 AI 诊断系统对疑似肺结节患者的诊断及对结节类型的评估价值。**方法**：选取 2019 年 12 月 -2020 年 12 月在我院进行 CT 检查的 358 例疑似肺结节患者，将其按照随机数字表法分为两组：对照组（放射科医生根据 CT 扫描结果，通过人工阅片分析记录检出结节数量和影像特征），观察组（将 CT 扫描结果导入 AI 辅助诊断系统，经 AI 运算得到结节检出数量和影像特征）。AI 辅助系统 IMsight 用于肺结节的图像分析和自动检测。通过组织病理学确定结节的良恶性。绘制受试者工作特征曲线（ROC）曲线以评估 AI 和 CT 结合图像的诊断价值。**结果**：病理结果最后确诊结节数量 736 个，恶性结节 139 个（18.89 %），良性结节 597 个（81.11 %）。观察组诊断结节数量 717 个，检出率 97.42%，对照组诊断出结节数量 603 个，检出率 81.93 %。观察组较对照组的结节检出率、阳性检出率升高（P<0.05），漏检率和假阴性率均显著降低（P<0.05）。当结节小于 10 mm 时，观察组较对照组的检出率升高（P<0.05），观察组较对照组对磨玻璃密度结节和实性结节检出率升高（P<0.05），观察组较对照组位于胸膜结节检出率升高（P<0.05）。观察组较对照组 AUC（P<0.05），表明 AI 系统下的结节检出准确率高。ROC 曲线显示观察组的敏感性和特异性分别为 88.39%和 89.68 %，对照组的敏感性和特异性分别为 75.24 %和 82.34 %，观察组较对照组的 ROC 曲线敏感性和特异性升高（P<0.05）。**结论**：AI 辅助诊断系统可有效提高肺结节的检出率，减少误检率及漏检率，值得在肺结节 CT 检测中应用推广。

关键词：胸部 CT；人工智能诊断；肺结节；诊断价值

中图分类号：R445；R563.9 **文献标识码**：A **文章编号**：1673-6273（2022）05-955-05

Chest CT Combined with AI Diagnosis System in the Diagnosis of Patients with Suspected Pulmonary Nodules and the Evaluation Value of Nodule Types*

LIU Ya-bin, LI Qing, ZHOU Wei, ZHENG Chang-jun, SHU Ya

(Department of Radiology, The First Affiliated Hospital of Chengdu Medical College, Chengdu, Sichuan, 610500, China)

ABSTRACT Objective: To investigate the diagnostic value of chest CT combined with AI diagnostic system in patients with suspected pulmonary nodules and the evaluation of nodule types. **Methods:** From December 2019 to December 2020, 358 patients with suspected pulmonary nodules who underwent CT examinations in our hospital were selected, and they were divided into two groups according to the random number table method: control group (radiologists used CT scan results to record the number of nodules and image characteristics through manual reading analysis) and observation group (import the CT scan results into the AI-assisted diagnosis system, and get the number of nodules detected and the image characteristics through AI calculations). All patients were examined by Siemens photonic dual-source CT. The AI assist system IMsight is used for image analysis and automatic detection of lung nodules. Determine the cancerousness of the nodule by histopathology. Draw a receiver-operator characteristic(ROC) curve to evaluate the diagnostic value of AI and CT combined images. **Results:** The pathological results finally confirmed 736 nodules, 139 malignant nodules (18.89 %), and 597 benign nodules (81.11 %). The number of nodules diagnosed in the observation group was 717, with a diagnosis rate of 97.42 %, and the number of nodules diagnosed in the control group was 603, with a diagnosis rate of 81.93 %. Compared with the control group, the nodule detection rate and positive detection rate of the observation group were higher (P<0.05), and both the missed detection rate and false negative rate are significantly reduced (P<0.05). When the nodule is smaller than 10mm, the detection rate of the observation group is higher than that of the control group (P<0.05), and compared with the control group, the observation group has higher detection rate of ground glass density nodules and solid nodules (P<0.05). Compared with the control group, the detection rate of nodules located in the middle of the pleura was higher (P<0.05). Compared with the control group, the observation group has a higher AUC (P<0.05), indicating that the detection accuracy of nodules under the AI system is higher. The ROC curve showed that the sensitivity and specificity of the ob-

* 基金项目：四川省医学科研课题计划项目（Q18005）

作者简介：刘亚斌（1982-），男，硕士，副主任医师，研究方向：胸腹部常见病及疑难病的影像诊断及鉴别诊断，

电话：13388164060，E-mail：liuyabin198206@163.com

（收稿日期：2021-08-03 接受日期：2021-08-27）

servation group were 88.39% and 89.68%, and the sensitivity and specificity of the control group were 75.24% and 82.34%, respectively. Compared with the control group, the sensitivity and specificity of the observation group were higher(P<0.05). **Conclusion:** The AI-assisted diagnosis system can effectively improve the detection rate of lung nodules, reduce the false detection rate and the missed detection rate, and it is worthy of application and promotion in CT detection of lung nodules.

Key words: Chest CT; AI diagnosis; Pulmonary nodules; Diagnostic value

Chinese Library Classification(CLC): R445; R563.9 Document code: A

Article ID: 1673-6273(2022)05-955-05

前言

肺癌是人类健康的主要威胁之一,其发病率和死亡率均居所有癌症之首,通常临床确诊时已达到中晚期,临床治疗效果不佳[1]。因此,肺癌的早期筛查和诊断尤为重要,是提高肺癌治疗效果的关键环节。对于肺结节的筛查,计算机断层扫描(Computer tomography,CT)是关键成像技术,而其他可用方法的重要性较低[2]。在医学图像分析中,必须在有限的时间内分析单个患者的大量图像,并识别所有肺结节并通过分析其边界、形状、位置和大小等影像学特征,以此归纳其影像类型(实性、部分实性或非实性)[3,4],以推测其良恶性,为临床治疗方案的制定提供依据。手动测量结节并作人工分析存在较大误差的可能,而早期发现、正确诊断和精准治疗肺癌,能从根本上延长患者的生存期,提高其生活质量[5]。基于胸部 CT 图像的人工智能(artificial intelligence,AI)技术在肺结节智能检测中的应用是该领域的热点问题,因此,深度学习 AI 肺结节辅助检测系统的出现是必然趋势[6,7]。相关研究表明,人工智能的肺结节辅助检测系统可以提高放射科医师的检测率和工作效率[8,9]。人工智能被用于医学的许多领域,包括医学诊断、医学统计、机器人技术和人类生物学,还可用作计算机辅助诊断系统,用于识别候选结节并检索尽可能多的诊断相关信息[10,11]。本研究以 358 例疑似肺结节患者为临床研究对象,探讨胸部 CT 结合 AI 诊断系统对肺结节诊断的价值。

1 资料与方法

1.1 一般资料

选取 2019 年 12 月 -2020 年 12 月在成都医学院第一附属医院因疑似肺结节进行 CT 检查的 358 例患者,其中男性患者 196 例,女性患者 162 例,平均年龄 54.27± 4.19 岁。根据实验目的分为两组:对照组(放射科医生根据 CT 扫描结果,通过人工阅片分析记录检出结节数量和影像特征),观察组(将 CT 扫描结果导入 AI 辅助诊断系统,经 AI 运算得到结节检出数量和影像特征)。

表 1 一般资料

Table 1 General Information

Project		n	Percentage(%)	t/x^2	P
Age (year of age)	18~35	83	23.18%	8.403	0.117
	36~65	167	46.65%		
	＞65	108	30.17%		
Gender	Male	208	58.10%	7.229	0.215
	Female	150	41.90%		
BMI(kg/m²)	＜22	97	27.09%	6.035	0.038
	22~24	173	48.32%		
	＞24	88	24.58%		
Smoke	Currently smoking	94	26.26%	6.142	0.026
	Smoking for nearly 6 years	76	21.23%		
	Never smoking	188	52.51%		
Family history of pulmonary disease	Yes	18	5.03%	5.374	0.012
	No	340	94.97%		

两组患者一般资料见表 1,差异无统计学意义(P＞0.05)。

1.1.1 **入组标准** 男女不限,18 岁以上;手术前 30 天内的肺部 CT 图像;CT 图像应为薄层水平序列 CT 图像(层厚 1.0~3.0 mm)。

1.1.2 **排除标准** CT 扫描不足(在结节上成像的噪声过多、运动伪影或边缘不足);当前或既往有恶性肿瘤史;诊断未知或无法确定;肺部弥漫性病变。

1.1.3 **医学伦理学问题** 本研究得到了本院审查委员会和医伦理委员会的批准,患者均知情同意本研究内容。

1.2 方法

1.2.1 **CT 扫描** 采用西门子 Definition AS + 64 排 128 层螺旋

CT 扫描仪。患者取仰卧位、双臂上举、头先进,均在吸气末屏气后扫描。扫描参数分别为:管电压 120 kV;管电流:自动管电流调制;螺距:1.2;层厚 5.0 mm;图像矩阵 512× 512;视野 326 mm。均使用标准算法重建 1.5 mm 层厚轴位图像。扫描范围从肺尖至肺底。运用肺窗进行图像分析 (窗宽 1600HU, 窗位－600 HU) 。

1.2.2 **图像分析** 两名胸部影像亚专业高年资放射科医师对对照组所有病例图像做人工阅片分析并记录影像分析结果,包括发现结节数量及影像学特征(位置,大小,衰减情况等)。另外由一名放射科医师将所有观察组病例图像导入 AI 系统, 并运行 3 次以上,然后记录 3 次运行结果中发现结节最多的一次为最终结果,包括发现结节数量及影像学特征(位置,大小,衰减情况等)AI 肺结节辅助检测系统 -IMsight 用于肺结节的图像分析和自动检测。然后将获得的观察组和对照组图数据进行统计学分析。

1.2.3 **结节性质确诊** 使用一种或多种方法确定每个结节的性质。所有恶性肿瘤都必须通过组织学证据证实。一些良性结节通过临床治疗后复查或者定期复查后缩小或者病灶消失来证实。

1.3 统计分析

所有结果均表示为例或者百分比。使用 SPSS 22.0 通过卡方检验确定组间统计显著性,统计显著性设置为 P<0.05。

2 结果

2.1 结节诊断详细统计

75 人(20.95%)确诊恶性结节。病理结果最后确诊结节数量 736 个, 恶性结节 139 个 (18.89%), 良性结节 597 个 (81.11%)。具体结节大小、结节密度值和结节毛刺详细统计见表 2。(表 2)。

表 2 结节诊断详细统计[n(%)]

Table 2 Detailed statistics of nodule diagnosis[n(%)]

Projec		Carcinoma	Optimum	Total
Gender	Male	81(11.01)	316(42.93%)	397(53.94%)
	Female	58(7.88)	281(38.18%)	339(46.06%)
Ncle size(mm)	5	6(0.82)	113(15.35)	119(16.17)
	5~7	12(1.63)	197(26.77)	209(28.40)
	7~10	33(4.48)	138(18.75)	171(23.23)
	10~15	88(11.96)	149(20.24)	237(32.20)
Ncle density value(HU)	0~80	57(7.74)	316(42.93)	373(50.68)
	80~300	82(11.14)	281(38.18)	363(49.32)
Tubercle burr	Yes	54(7.34)	526(71.47)	580(78.80)
	No	85(11.55)	719(9.65)	156(21.20)

2.2 阳性结节检出率比较

观察组较对照组的结节检出率、阳性检出率升高(P<0.05),漏检率和假阴性率降低(P<0.05)。(表 3)。

表 3 阳性结节检出率比较

Table 3 Comparison of detection rate of positive nodules

Indicators	Control group	Observation group	x^2	P
Check-Out Rate(%)	603(81.93 %)	717(97.42 %)	6.533	0.006
Leak detection rate(%)	133(18.07 %)	19(2.58 %)	7.184	0.033
Positive Rate(%)	123(88.40 %)	134(96.40 %)	6.297	0.025
False negative rate(%)	16(11.51 %)	5(3.59 %)	5.867	0.014

2.3 结节特征诊断结果比较

当结节小于 10 mm 时, 观察组较对照组的检出率升高(P<0.05),观察组较对照组磨玻璃密度结节和实性结节的结节检出率升高(P<0.05),观察组较对照组对胸膜结节检出率升高(P<0.05)。(表 4)。

2.4 CT 与 AI 结合对结节诊断准确率评估

通过计算 ROC 曲线下面积(AUC)评两种方法对结节诊断的准确率,观察组 AUC 较对照组显著增加(P<0.05)。

图 2 显示了 ROC 曲线说明了对照组和观察组中检测肺结节的诊断性能。(图 2,表 5)。

2.5 ROS 曲线的敏感特异性分析

观察组较对照组的 ROC 曲线敏感性和特异性显著增加(P<0.05)。(表 6)。

表 4 结节特征诊断结果比较

Table 4 Comparison of nodule characteristics diagnosis results

Ncle characteristics		n	Control group(%)	Observation group(%)	x^2	P
Ncle Size (mm)	5	119	45(37.82)	108(90.76)	6.926	0.001
	5~7	209	188(89.95)	202(96.65)		
	7~10	171	135(78.95)	170(99.42)		
	10~15	237	235(99.16)	237(100.00)		
Ncle status	Entity	325	284(87.38)	318(97.85)	5.714	0.004
	Part of the entity	48	46(95.83)	44(91.67)		
	Frosted glass	363	273(75.21)	355(97.80)		
Nocle location	Middle of the pleural membrane	517	406(78.53)	516(99.81)	9.533	0.006
	Surrounding and others	219	197(89.95)	201(91.78)		

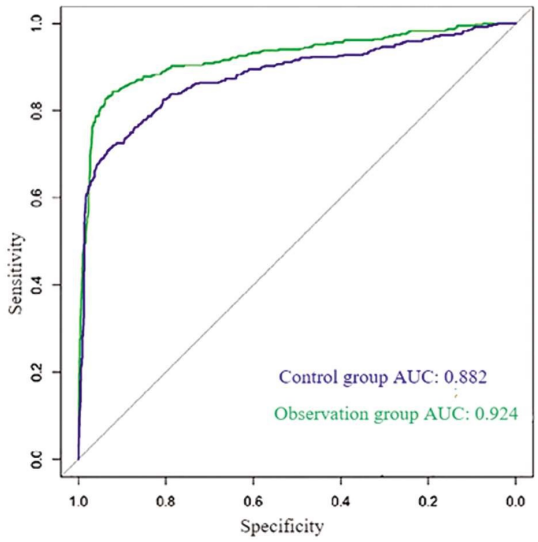

图 2 ROC 曲线分析

Fig.2 ROC curve analysis

3 讨论

人工智能被定义为计算机科学的一门学科,其重点是创造能够感知世界并与人类相似的机器[12]。最初用于简单数据分析的 AI 算法是由程序员硬编码的,无法识别非专门编程的模式。机器学习是 AI 的一个子领域，其中算法可以识别和学习复杂数据集中的模式以产生智能预测,而不是通过显式编程[13]。然而,大多数传统机器学习算法仍然需要人工输入,并且此类算法能够评估的模式仍然相当简单。深度学习可以被概念化为一类机器学习,其中算法被组织成许多基于人工神经网络的处理层,类似于人脑[14]。由于深度学习在许多计算机视觉任务中都表现出较高的准确率,近年来,基于深度神经网络的肺结节检测与分类研究领域迅速升温[15]。近年来,人工智能辅助的结节分割、检测和分类取得了很大进展,然而,用于结节评估的机器学习还处于起步阶段,仍有许多限制需要克服。

表 5 CT 与 AI 结合对结节诊断准确率评估

Table 5 Evaluation of Accuracy of Nodule Diagnosis by Combination of CT and AI

Project	Control group	Observation group	x^2	P
	CI 95 %(0.921-0.963)	CI 95 %(0.829-0.914)	9.426	0.002
AUC	0.882	0.924		

表 6 ROS 曲线的敏感特异性分析

Table 6 Sensitivity and specificity analysis of ROS curve

Project	Control group	Observation group	x^2	P
Sensitivity	75.24 %	88.39 %	6.533	0.006
Specific	82.34 %	89.68 %	5.867	0.014

与信息检索、分类、识别、翻译等相关的深度学习领域中最基本的两个指标是召回率和准确率[16]。召回率是医学诊断中的敏感性,但准确率并不具体。尽管如此,准确率和召回率之间的关系类似于敏感性和特异性之间的关系:准确率和召回率相互影响,理想情况当然是高精度和召回率,但一般情况下,查准率与查全率成反比[17]。本研究通过对诊断结果的分析表明:观察组 ROC 曲线对应的 AUC 值为 0.924,对照组则为 0.882,说明该模型对测试数据集中结节的诊断诊断价值较高,Singh R[18]和 Rampinelli C[19]等研究显示:临床医生诊断肺结节时,敏感性和特异性一般会比 AI 模型低，因此在自动机器学习系统的帮助

下,临床医生可以在没有深度学习专家帮助的情况下创建深度学习肺结节病理分类模型，该模型的诊断效率不亚于临床医生,但深度学习算法模型不会取代临床医生和放射科医生的地位,相反,AI 可以有效地帮助临床医生和放射科医生进行临床诊断工作[18,19]。鉴于体积 CT 具有超过 900 万个体素,而一个 5 毫米结节仅占据大约 130 个体素,因此在 CT 上检测小肺结节可能具有挑战性。多项研究表明,放射科医生之间的结节检测灵敏度存在显著差异，国家肺筛查试验中漏检的癌症高达 8.9%[20,21]。

肺结节的传统计算机辅助算法包括结节分割、特征提取、将病变分类为非结节而不是真正的结节[22-24]。所选特征的数量和用于分类的机器学习模型类型取决于所使用的计算机辅助系统的类型。尽管传统计算机学习辅助成功地辅助了结节检测,但传统机器学习的一个缺陷是过度拟合。使用深度学习的算法可能会消除传统计算机辅助系统中的先天障碍,因为它不需要复杂的人为主导的管道及其在有限的直接监督下自学习以前未知特征的能力。一项深度学习肺结节检测系统结果显示,报告灵敏度为 73%,特异性为 80%,优于当时可用的传统 AI 系统[25]。并且有多项研究[26-28]表明深度学习的计算机辅助比传统 AI 具有优越性，与本研究结果一致。相关研究使用 LUNA 16 和 Ali Tianchi 数据库开发了一个用于检测肺结节的 AI 网络,并评估了其在 LUNA 16 数据集上的性能,结果其扫描的灵敏度分别高达 81.7% 和 85.1%[29]，与本研究数据较为接近。但也有研究[30]显示结节检测的灵敏度高达 95 %,略高于本研究结果,分析其原因在于:该研究样本量比本研究少近一倍,因此相对而言该研究可能存在一定偏倚性,导致数据结果偏高。

综上所述，我们的研究表明 AI 辅助诊断系统可有效提高肺结节的检出率,减少误检率及漏检率,值得在肺结节 CT 检测中应用推广。

参 考 文 献(References)

[1] Pezeshk A, Hamidian S, Petrick N, et al. 3-D Convolutional Neural Networks for Automatic Detection of Pulmonary Nodules in Chest CT[J]. IEEE J Biomed Health Inform, 2019, 23(5): 2080-2090

[2] Gruden JF, Naidich DP, Machnicki SC, et al. An Algorithmic Approach to the Interpretation of Diffuse Lung Disease on Chest CT Imaging: A Theory of Almost Everything [J]. Chest, 2020, 157(3): 612-635

[3] Gong L, Jiang S, Yang Z, et al. Automated pulmonary nodule detection in CT images using 3D deep squeeze-and-excitation networks[J]. Int J Comput Assist Radiol Surg, 2019, 14(3): 1969-1979

[4] 陈雷,盖虎支,张郁,等. 16 层螺旋 CT 不同剂量扫描对肺结节诊断价值及辐射度的影响 [J]. 现代生物医学进展, 2020, 20(11): 2139-2142

[5] Milanese G, Silva M, Frauenfelder T, et al. Comparison of ultra-low dose chest CT scanning protocols for the detection of pulmonary nodules: a phantom study[J]. Tumori, 2019, 105(5): 394-403

[6] Tosi D, Mendogni P, Carrinola R, et al. CT-guided fine-needle aspiration biopsy of solitary pulmonary nodules under 15 mm in diameter: time for an afterthought[J]. J Thorac Dis, 2019, 11(3): 724-731

[7] Choe J, Lee SM, Do KH, et al. Deep Learning-based Image Conversion of CT Reconstruction Kernels Improves Radiomics Reproducibility for Pulmonary Nodules or Masses[J]. Radiology, 2019, 292(2): 365-373

[8] Wu G, Woodruff HC, Shen J, et al. Diagnosis of Invasive Lung Adenocarcinoma Based on Chest CT Radiomic Features of Part-Solid Pulmonary Nodules: A Multicenter Study [J]. Radiology, 2020, 297(2): 451-458

[9] Ohno Y, Aoyagi K, Yaguchi A, et al. Differentiation of Benign from Malignant Pulmonary Nodules by Using a Convolutional Neural Network to Determine Volume Change at Chest CT[J]. Radiology, 2020, 296(2): 432-443

[10] Rosenkrantz AB, Xue X, Gyftopoulos S, et al. Downstream Costs Associated with Incidental Pulmonary Nodules Detected on CT[J]. Acad Radiol, 2019, 26(6): 798-802

[11] Gu X, Xie W, Fang Q, et al. The effect of pulmonary vessel suppression on computerized detection of nodules in chest CT scans [J]. Med Phys, 2020, 47(10): 4927

[12] Li WJ, Chu ZG, Zhang Y, et al. Effect of Slab Thickness on the Detection of Pulmonary Nodules by Use of CT Maximum and Minimum Intensity Projection[J]. AJR Am J Roentgenol, 2019, 213(3): 562-567

[13] Liu B, Chi W, Li X, et al. Evolving the pulmonary nodules diagnosis from classical approaches to deep learning-aided decision support: three decades' development course and future prospect [J]. J Cancer Res Clin Oncol, 2020, 146(1): 153-185

[14] Baldwin DR, Gustafson J, Pickup L, et al. External validation of a convolutional neural network artificial intelligence tool to predict malignancy in pulmonary nodules[J]. Thorax, 2020, 75(4): 306-312

[15] Wang J, Chen X, Lu H, et al. Feature-shared adaptive-boost deep learning for invasiveness classification of pulmonary subsolid nodules in CT images[J]. Med Phys, 2020, 47(4): 1738-1749

[16] Chen G, Zhang J, Zhuo D, et al. Identification of pulmonary nodules via CT images with hierarchical fully convolutional networks[J]. Med Biol Eng Comput, 2019, 57(7): 1567-1580

[17] Liang CH, Liu YC, Wu MT, et al. Identifying pulmonary nodules or masses on chest radiography using deep learning: external validation and strategies to improve clinical practice [J]. Clin Radiol, 2020, 75(1): 38-45

[18] Singh R, Digumarthy SR, Muse VV, et al. Image Quality and Lesion Detection on Deep Learning Reconstruction and Iterative Reconstruction of Submillisievert Chest and Abdominal CT [J]. AJR Am J Roentgenol, 2020, 214(3): 566-573

[19] Rampinelli C, Cicchetti G, Cortese G, et al. Management of incidental pulmonary nodule in CT: a survey by the Italian College of Chest Radiology[J]. Radiol Med, 2019, 124(7): 602-612

[20] Mazzone PJ, Gould MK, Arenberg DA, et al. Management of Lung Nodules and Lung Cancer Screening During the COVID-19 Pandemic: CHEST Expert Panel Report[J]. Chest, 2020, 158(1): 406-415

[21] Araujo-Filho JAB, Halpenny D, McQuade C, et al. Management of Pulmonary Nodules in Oncologic Patients: AJR Expert Panel Narrative Review[J]. AJR Am J Roentgenol, 2021, 216(6): 1423-1431

[22] Harada M, Aono Y, Yasui H, et al. Minute Pulmonary Meningothelial-like Nodules Showing Multiple Ring-shaped Opacities [J]. Intern Med, 2019, 58(21): 3149-3152

(下转第 949 页)

[10] Condò V, Cipriani S, Colnaghi M, et al. Neonatal respiratory distress syndrome: are risk factors the same in preterm and term infants?[J]. J Matern Fetal Neonatal Med, 2017, 30(11): 1267-1272

[11] 阎丽华, 宁伟伟, 江倩男, 等. 呼吸窘迫综合征早产儿血清 VA、PCT、TNF-α 及 CRP 水平的表达及临床意义 [J]. 现代生物医学进展, 2019, 19(20): 3943-3946

[12] Matthay MA, Zemans RL, Zimmerman GA, et al. Acute respiratory distress syndrome[J]. Nat Rev Dis Primers, 2019, 5(1): 18

[13] Dembinski R, Mielck F. ARDS - An Update - Part 1: Epidemiology, Pathophysiology and Diagnosis [J]. Anasthesiol Intensivmed Notfallmed Schmerzther, 2018, 53(2): 102-111

[14] Climent M, Viggiani G, Chen YW, et al. MicroRNA and ROS Crosstalk in Cardiac and Pulmonary Diseases[J]. Int J Mol Sci, 2020, 21(12): 4370

[15] Rajasekaran S, Pattarayan D, Rajaguru P, et al. MicroRNA Regulation of Acute Lung Injury and Acute Respiratory Distress Syndrome [J]. J Cell Physiol, 2016, 231(10): 2097-2106

[16] Maroof H, Islam F, Dong L, et al. Liposomal Delivery of miR-34b-5p Induced Cancer Cell Death in Thyroid Carcinoma [J]. Cells, 2018, 7 (12): 265

[17] Dong L, Chen F, Fan Y, et al. MiR-34b-5p inhibits cell proliferation, migration and invasion through targeting ARHGAP1 in breast cancer [J]. Am J Transl Res, 2020, 12(1): 269-280

[18] Wang Z, Zhang X, Li Z, et al. MiR-34b-5p Mediates the Proliferation and Differentiation of Myoblasts by Targeting IGFBP2 [J]. Cells, 2019, 8(4): 360

[19] Jang H, Park S, Kim J, et al. The Tumor Suppressor, p53, Negatively Regulates Non-Canonical NF-κB Signaling through miRNAInduced Silencing of NF-κB-Inducing Kinase [J]. Mol Cells, 2020, 43 (1): 23-33

[20] 艾再提·克热木, 阿地力江·萨吾提, 艾尼瓦尔·吾买尔. 核因子 -κB 的研究现状[J]. 西北药学杂志, 2020, 35(1): 143-148

[21] Hu RP, Lu YY, Zhang XJ. MiR-34b-5p knockdown attenuates bleomycin-induced pulmonary fibrosis by targeting tissue inhibitor of metalloproteinase 3 (TIMP3)[J]. Eur Rev Med Pharmacol Sci,2019, 23(5): 2273-2279

[22] Du X, Yang Y, Xiao G, et al. Respiratory syncytial virus infection-induced mucus secretion by down-regulation of miR-34b/c-5p expression in airway epithelial cells [J]. J Cell Mol Med, 2020, 24 (21): 12694-12705

[23] Bayraktar R, Van Roosbroeck K. miR-155 in cancer drug resistance and as target for miRNA-based therapeutics [J]. Cancer Metastasis Rev, 2018, 37(1): 33-44

[24] Wang C, Zhang C, Liu L, et al. Macrophage-Derived mir-155-Containing Exosomes Suppress Fibroblast Proliferation and Promote Fibroblast Inflammation during Cardiac Injury [J]. Mol Ther, 2017, 25 (1): 192-204

[25] Li GS, Cui L, Wang GD. miR-155-5p regulates macrophage M1 polarization and apoptosis in the synovial fluid of patients with knee osteoarthritis[J]. Exp Ther Med, 2021, 21(1): 68

[26] Bala S, Csak T, Saha B, et al. The pro-inflammatory effects of miR-155 promote liver fibrosis and alcohol-induced steatohepatitis [J]. J Hepatol, 2016, 64(6): 1378-1387

[27] Fu X, He HD, Li CJ, et al. MicroRNA-155 deficiency attenuates inflammation and oxidative stress in experimental autoimmune prostatitis in a TLR4-dependent manner [J]. Kaohsiung J Med Sci, 2020, 36 (9): 712-720

[28] Jiang K, Yang J, Guo S, et al. Peripheral Circulating Exosome-Mediated Delivery of miR-155 as a Novel Mechanism for Acute Lung Inflammation[J]. Mol Ther, 2019, 27(10): 1758-1771

[29] Li HF, Wu YL, Tseng TL, et al. Inhibition of miR-155 potentially protects against lipopolysaccharide-induced acute lung injury through the IRF2BP2-NFAT1 pathway [J]. Am J Physiol Cell Physiol, 2020, 319(6): C1070-C1081

[30] Yan Y, Lou Y, Kong J. MiR-155 expressed in bone marrow-derived lymphocytes promoted lipopolysaccharide-induced acute lung injury through Ang-2-Tie-2 pathway [J]. Biochem Biophys Res Commun, 2019, 510(3): 352-357

（上接第 959 页）

[23] Fletcher JG, Levin DL, Sykes AG, et al. Observer Performance for Detection of Pulmonary Nodules at Chest CT over a Large Range of Radiation Dose Levels[J]. Radiology, 2020, 297(3): 699-707

[24] 李凤芝, 王东, 毕永民, 等. 39 例飞行人员肺结节临床特点及诊治初探[J]. 国际呼吸杂志, 2021, 41(05): 378-383

[25] Yarmus L, Akulian J, Wahidi M, et al. A Prospective Randomized Comparative Study of Three Guided Bronchoscopic Approaches for Investigating Pulmonary Nodules: The PRECISION-1 Study [J]. Chest, 2020, 157(3): 694-701

[26] Gu X, Wang J, Zhao J, et al. Segmentation and suppression of pulmonary vessels in low-dose chest CT scans [J]. Med Phys, 2019, 46 (8): 3603-3614

[27] Wu W, Gao L, Duan H, et al. Segmentation of pulmonary nodules in CT images based on 3D-UNET combined with three-dimensional conditional random field optimization [J]. Med Phys, 2020, 47 (9): 4054-4063

[28] Meltzer C, Fagman E, Vikgren J, et al. Surveillance of small, solid pulmonary nodules at digital chest tomosynthesis: data from a cohort of the pilot Swedish CArdioPulmonary bioImage Study (SCAPIS)[J]. Acta Radiol, 2021, 62(3): 348-359

[29] Zhang C, Sun X, Dang K, et al. Toward an Expert Level of Lung Cancer Detection and Classification Using a Deep Convolutional Neural Network[J]. Oncologist, 2019, 24(9): 1159-1165

[30] 李欣菱. 基于深度学习的人工智能胸部 CT 肺结节检测效能评估 [D]. 天津医科大学, 2020